



Electrochemical and Surface Characterization of *Chondria Macrocarpa* Extract (CME) as Save Corrosion Inhibitor for Aluminum in 1M HCl Medium

A. S. Fouda¹*, N. E. Al-Hazmi², H. H. El-Zehry³ and A. El-Hossainy^{1,4}

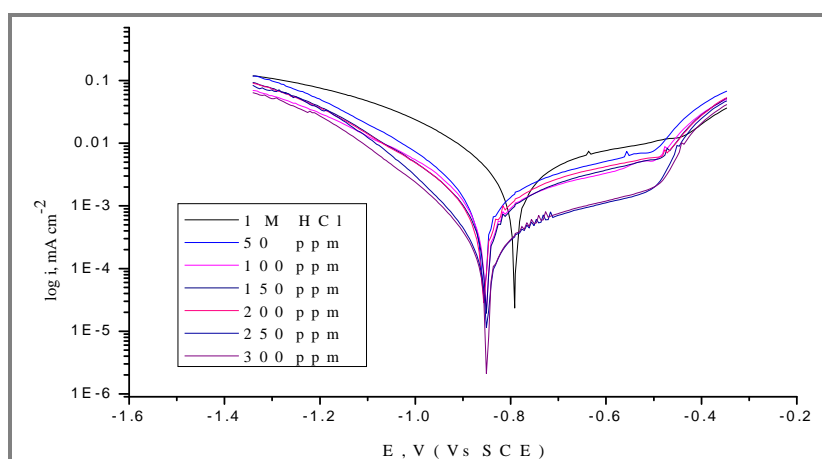
1. Chemistry Department, Faculty of Science, Mansoura University, Mansoura-35516, **EGYPT**
 2. University college of Qunfudah, Umm Alqura University, Mecca, Kingdom, **SAUDI ARABIA**
 3. Al-Qunfudah Medical College, Umm Al Qura University, Mecca, **SAUDI ARABIA**
 4. Chemist, Delta Fertilizers Company in Talkha, **EGYPT**
- Email: asfouda@hotmail.com

Accepted on 5th April, 2020

ABSTRACT

The examination of the effect of *Chondria Macrocarpa* Extract (CME) against the corrosion of Al in the acidic medium (1M HCl) was utilized via electrochemical and gravimetric determinations. The protection efficiency of CME was in 318 K for 300 ppm equal to 90.1% referring that it is highly recommended for utilizing for corrosion protection. The adsorption isotherm followed Langmuir. CME acts as mixed kind inhibitor and it was deduced from Tafel extrapolations. The thermodynamic parameters were tabulated and interpreted. The net result from the protection process, which was a fine film on Al surface, was inspected via Attenuated total reflection (ATR), Atomic forced microscopy (AFM).

Graphical Abstract



Potentiodynamic Polarization curve for corrosion of Al with and without different concentrations of inhibitor.

Keywords: Adsorption, *Chondria Macrocarpa*, Aluminum, HCl, Corrosion inhibition, AFM.

INTRODUCTION

Corrosion is the loss of metal characteristics by the time owing to surrounding environmental impacts to be in the most stable form. HCl is the corrosive medium of this study. It was chosen with a fixed dose which is 1M owing to it is the dose widely utilized in the industry. HCl is pickle liquor, ant scales, de-rusting, utilized in refining, cleaning, deposits removal [1-6]. The reaction of HCl with Al liberates H₂ gas can be observed very well by our eyes as it occurs forcefully. Aluminum (Al) has a self-protection feature towards the oxidation by the atmosphere. It can be interpreted by knowing that corrosion potential = -1.66 V so a fine layer spontaneously established. This means also it is easily corroding in destructive mediums, so it is indeed our need to save money and time in repairing every damage outcome from its corrosion. The plant extracts [7-13] are the new trend of protection process, cause by trier it was deduced that organic inhibitor really so effective but also unfriendly and toxic. The plant extracts proved highly protection and a natural alternate of the organic inhibitors and contains the same constituents. Al has several applications, among this apps: architecture; (aquatic centers& Banks) due to docile strong, flexible, characteristics; transportation apps owing to strength under pressure and light weight; electrical apps (sound systems, satellite dishes) owing to it's very good standards of corrosion resistance [14, 15]; consumer apps (foils, beverages, refrigerators, laptops, smart phones) [16] owing to it is suitable conductor [17] for heat and aids in keeping electronic devices from being hotter. The objective of this study is using *CME* as a new save corrosion inhibitor for Al in HCl solution at different concentrations and temperatures.

MATERIALS AND METHODS

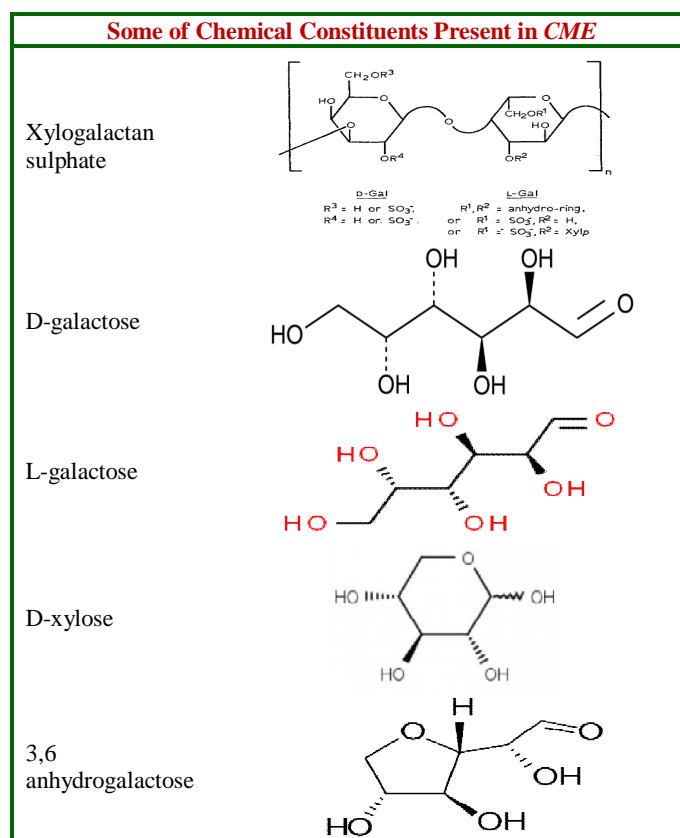
The model of Al samples for the chemical assessments was the squares with 20 mm for its length and 20 mm for its width and 0.2 cm for its thickness, designed by wire apparatus to keep away from the un-equal angles, misrepresentation of lattice structure of the samples gained from other cutting methods, with the Al content of 99.9 %, the same model were utilized for the surface surveys. The model of the working electrode was 1cm x 1cm welded to the Cu wire via Sn then surrounded by glass tube fitted with epoxy, then stay for one day to have the acquired suitable cohering. The samples treated with mechanical abrasion with diverse levels of silicon carbide sheets (320-1200) till having a mirror view, then with deionized water, then acetone.

An appropriate concentration of 37 % HCl (1M) was prepared in bidistilled water and titrated vs. 1M Na₂CO₃. The concentration range of the *CME* was varied from 50 to 300 ppm and they prepared closely before utilizing.

Samples of the plant were taken after drying, grinder to powder shape then extracted utilizing the bidistilled water. Then, adding 0.1 Kg of the net volume to 250 ml of bidistilled water at 353K for 40 minutes, then left for one day, and water-filtered by a filter paper utilizing glass funnel, filled to the net volume of the flask by bidistilled water, the final step is stocking, preserving in one of suitable cooling systems in glass flask [18].

Chondria is a red alga genus in the family Rhodomelaceae. The phytochemical screening of the *Chandra Macrocarpa* (*CME*) confirmed the presence of various organic compounds. The major compounds are the highly acidic xylogalactan sulphate [19], also contains other major constituents such as D-galactose, L-galactose, D-xylose, 3, 6 anhydrogalactose.

Weight loss (WL) procedure: Assessments of WL utilized samples with magnitude of (20 mm x 20 mm x 0.2 cm). The samples were abraded one immediately after the other successively with different progression of emery sheets of different levels beginning with the 320 to 1200 level, dry-cleansed with acetone likewise air-dried, then weighed. The mass loss experiment was complemented in a 100 mL 1 M HCl mixtures with and without diverse doses of *CME*. The ratios of dissolution were assessed utilizing the closest equation [20]:

Table 1. List of the serious phytochemical constituents in *CME*

$$(CR) = \Delta m / st \quad \dots(1)$$

The loss of the mass is signified as Δm , the surface area of the samples exposed to the solution (cm^2) is signified as s , and the submergence time is signified as t . The inhibition efficiency or (protection efficiency) is signified as %IE and surface coverage signified as θ , were assessed utilizing the closest equation:

$$\%IE = \theta \times 100 = 1 - [CR_{inh}/CR_{corr}] \times 100 \quad \dots(2)$$

The dissolution ratios of Al with and without *CME* were signified as CR_{inh} and CR_{corr} .

Hydrogen evolution (HE) procedure: The samples utilized in this procedure are the same of the WL procedures. The same treatment for the gravimetric procedure also implemented here. The samples were submerged in a 100 mL closed bottle comprising the prepared solution. H_2 gas evolved and gathered through tube attached to a gas burette firmly resolved in a beaker stuffed with water. The switch of the volume produced by air compression. This permitted assessment of the volume of gas evolved corresponding to the time. The experimental solution was procedure in attendance and non-attendance of the diverse doses of *CME*. The (%IE) was assessed utilizing the closest equation:

$$\%IE = [R_B - R_E] / [R_B] \times 100 \quad \dots(3)$$

Behold, R_B and R_E are the dissolution ratio without and with *CME*, separately [21].

Acidification procedure: The pH was inspected for the experimental solution and the six doses 50, 100, 150, 200, 250 and 300 ppm pre and post submergence in the inspected solution for 3 hrs. The %IE assessed by implementing in the closest equation

$$[\text{H}^+]_{inh} / [\text{H}^+]_{uninh} \times 100 \quad \dots (4)$$

Where ΔH^+_{inh} and ΔH^+_{uninh} are changes in H^+ concentration in the attendance and non- attendance of *CME*, separately [22].

Potentiodynamic Polarization (PP) procedure: Analyses were procedure via the three-electrode cell assembly utilizing the reference electrode, the counter electrode, and the working electrode. The working electrode was designed from the same samples utilized in chemical procedures; the area of exposed surface positions was 1 cm^2 . The electrode surface was processed with the same treatment of the gravimetric method earlier the trials. Subsequently, the electrode was submerged in experimental solution at the open-circuit potential (OCP) for half an hour till a steady state was ended. Assessments taken as a function of current densities, the %IE for each dose of the *CME* was assessed utilizing the closest equation [23]:

$$\% IE = \Theta \times 100 = 1 - [i_{inh}/i_{corr}] \times 100 \quad \dots (5)$$

Behold, i_{corr} and i_{inh} are the dissolution current densities assessed from the Tafel slopes without-attendance and with- attendance of *CME*.

Alternating current impedance spectra (EIS) procedure: The (EIS) was performed via the three-electrode cell management utilizing the reference electrode, the counter electrode, and the working electrode. The same treatment for the working electrode in PP was implemented. EIS assessments were proved utilizing AC signals with an amplitude of 5 mV peaks at the open circuit potential (OCP) in the frequency range of 100 kHz to 0.1 Hz. All impedance outcomes were consented to the convenient equivalent circuit utilizing the software of Gamry Echem Analyst, the protection efficiency %IE was assessed corresponding to R_{ct} [24].

Electrochemical frequency modulation (EFM) procedure: EFM procedure is regarded as quick, non-ruinous and dependable electrochemical method. Terminating signals with amplitude 10 mV to 2 and 5 Hz is the way to implement the interrogation where, the current density signified as (i_{corr}), the Tafel slopes signified as (β_c and β_a) and the causality factors as (CF-2 and CF-3) can be immediately assessed from the higher peaks [25]. The apparatus utilized in EFM interrogations was the Gamry (Potentiostat/Galvanostat/ZRA (PCI4-G750). Gamry software description comprises DC105 software for DC corrosion, EIS 300 software for electrochemical impedance spectroscopy and EFM 140 for electrochemical frequency modulation assessments as well as a computer for data picking up. Echem analyst version 5.5 software was utilized for scheming, figuring and fitting data. The protection efficiency %IE assessed according to the i_{corr} .

ATR-FTIR and UV/Visible Spectral Analysis: Attenuated total reflection (ATR) Inspection gives a qualitative characterization of the *CME* adsorption on the Al surface via recognizing the functional groups settled on the surface [26]. Al samples submerged in the experimental solution whole a day (24 h) with and without the *CME*, Post submerging duration the samples inspected by (Thermo Fisher scientific IS-10 FT-IR and ATR) to survey the feature of the film settled on the surface of the samples. The experimental solution containing *CME* after submerging of Al samples for a day (24 h) was inspected on (PG UV/Vis Spectrophotometer T80+) also pure *CME* was inspected by the same apparatus.

AFM Analysis: Atomic Forced Microscopy (AFM) technique is a procedure to inspect the morphological features of Al surface in experimental solution without and with *CME*. The samples of Al were treated alike gravimetric method and submerged in the experimental solution without and with 300 ppm of the *CME* for a day (24 h) at 298K. After this duration, the samples were exerted out of the solution, carefully rinsed utilizing deionized water then dried by air dryer [27]. The surface inspection was utilizing AFM was processed in contact mode utilizing Silicon Nitride probe model

MLCT produced by Bruker. Proscan 1.8 software utilized to control the scan parameters and IP 2.1 software for image analysis. Scan parameters: scan area: $-10 \times 10 \mu\text{m}^2$, scan rate: 1 Hz. Number of data points: The measured area divided into 256 lines and every line divided into 256 points. The scanned area is $2 \mu\text{m}$ per division, they are 5 divisions, so it is equal = $10 \mu\text{m} \times 10 \mu\text{m}$.

Assessment the Inhibition of CME against Microbial Growth: CME was utilized for testing its ability to prohibit the growth of bacteria in cooling tower of ammonia at Talkha factory for fertilizers by implementing the spore suspension procedure. By separating this bacterium and cultivate it in a plate over nutrient agar then after growth, taking several swaps from several collected colonies then multiply it in 1L measuring flask containing deionized water. Then left it for 1-3/2h before cultivating again (with adding CME). After waiting time, pouring from it to a 100 ml flask containing 10 mL of HCl and 30 mL of CME then completing to 100 mL. Then left it for 1/2 -1h then taking 2 mL from this solution by syringe and pouring over agar solution in two cultivating plates; one is containing the pure CME, the other containing the 300 ppm and waiting for maximum 2 days. The plates were incubated at 310K then counting colonies by UVP colony DOC-It apparatus, the plates exhibited suitable resistance to the bacteria.

RESULTS AND DISCUSSION

Weight Loss assessments: Every half an hour WL of Al samples was sharply followed (30, 60, 90, 120, 150 and 180 min) at fixed temperatures, raising 5 temperatures from the previous one starting from 298 K then (303, 308, 313 and 318 K); WL graphical representation at 298 K is here in figure 1. The protection efficiency %IE at different temperatures is submitted in table 2. The impact of temperature on % IE is viewed in figure 2. The outcomes detected that the addition of CME diminishes the ratios of Al dissolution. The %IE was deducted to be directly proportional to the dose raising of CME as in table 2. This owing to the adsorption of CME particles on the Al surface. These adsorbates diminish the Al destruction by blocking the corrosion sites as the dose of the CME raises, so raising the protection efficiency.

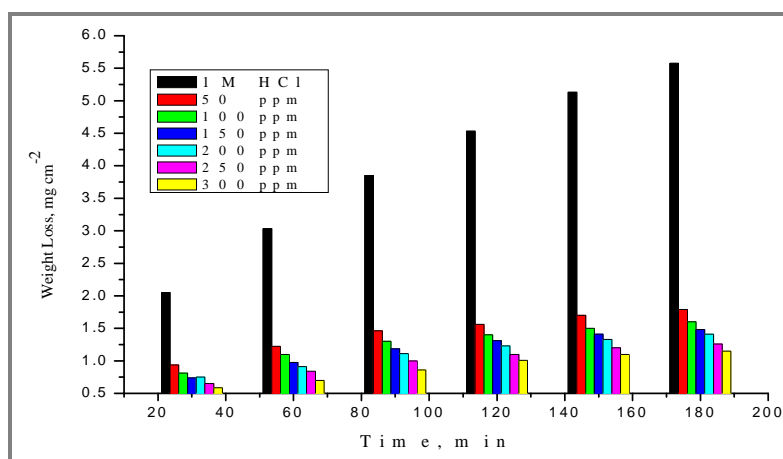


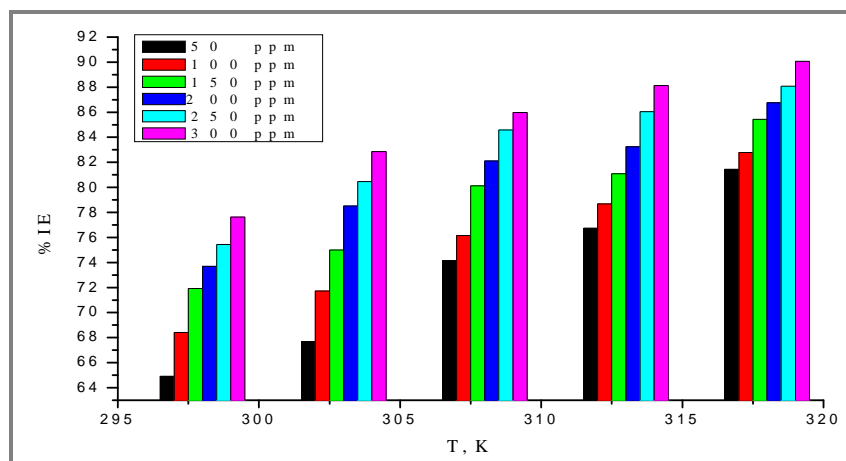
Figure 1. Graph of WL against time for Al in 1M HCl (experimental solution) in case of the experimental solution and in with diverse doses of CME at 298 K.

Adsorption Isotherms: The adsorption arrangement (chemical or physical adsorption) can be known by the application of adsorption isotherm [28]. WL procedure can evaluate θ which is a function of CME doses then graphed to fit appropriate kind of adsorption to measure the adsorption isotherms [29]. Calculations of the varied isotherms (Frumkin, Langmuir, Temkin, and Freundlich) referred that Langmuir adsorption isotherm figure 3 was the best, it exhibits a straight-line relation between C/θ and C [30]:

$$C/\theta = 1/K + C \quad \dots(6)$$

Table 2. Effect of addition of diverse doses of *CME* on the surface coverage (θ) and protection efficiency values (%*IE*) at diverse temperatures

Temp. (K)	Conc. (ppm)	<i>CME</i>	
		θ	% <i>IE</i>
298	50	0.646	64.6
	100	0.687	68.7
	150	0.708	70.8
	200	0.729	72.9
	250	0.750	75.0
	300	0.771	77.1
303	50	67.8	0.678
	100	71.2	0.712
	150	74.6	0.746
	200	76.3	0.763
	250	78.0	0.780
	300	79.7	0.797
308	50	73.8	0.738
	100	76.2	0.762
	150	79.8	0.798
	200	82.1	0.821
	250	83.3	0.833
	300	84.5	0.845
313	50	76.8	0.768
	100	78.7	0.787
	150	81.5	0.815
	200	83.3	0.833
	250	86.1	0.861
	300	87.0	0.870
318	50	81.4	0.814
	100	82.8	0.828
	150	85.4	0.854
	200	86.7	0.867
	250	88.1	0.881
	300	90.1	0.901

**Figure 2.** Effect of temperature on %*IE* utilizing diverse doses of *CME* on Al surface in 1M HCl (experimental solution).

Where the *CME* concentration signified as *C*, the adsorptive equilibrium constant signified as K_{ads} and can be accessed from the intercept of Langmuir isotherm in figure 3. The ΔG°_{ads} can be evaluated from Eq. 7, where, (ΔG°_{ads}) is standard free energy. Figure 4 exhibits the variation of $\log K_{ads}$ and $1/T$. The slope of the line gives the ΔH°_{ads} by applying in Eq 8

$$K_{ads} = 1/55.5 \exp [-\Delta G^{\circ}_{ads}] / RT \quad \dots(7)$$

Where R is the universal gas constant, T is the absolute temperature and 55.5 is the molar concentration of water in M^{-1} . By applying in Vant't Hoff equation ΔH_{ads}° can be evaluated as follow:

$$\log K_{ads} = \Delta H_{ads}^{\circ} / 2.303RT + \text{constant} \quad \dots(8)$$

Substituting in eq 9 from the values of ΔG_{ads}° & ΔH_{ads}° , ΔS values can be obtained

$$\Delta G_{ads}^{\circ} = \Delta H_{ads}^{\circ} - T\Delta S_{ads}^{\circ} \quad \dots(9)$$

The negative sign of ΔG_{ads}° support the spontaneous adsorption of the *CME* particles on the surface of Al. Hence, the results of ΔG_{ads}° was 36.6- 41.0 kJ mol^{-1} table 3, refers the suggested chemisorption adsorption. Where ΔG_{ads}° results up to -20 kJ mol^{-1} is assisting the physisorption mechanism while that around -40 kJ mol^{-1} assigns chemisorption adsorption [31]. The experimental results fit the utilized adsorption isotherm where the correlation coefficients (R^2) near to 1. The K values raises with raising in temperature table 3. K value points to the strength between adsorbent and adsorbate [32], its ranges raises with raising temperature, and this confirms the chemical mechanism. An exothermic adsorption ($\Delta H_{ads}^{\circ} < 0$) may include either physical adsorption or chemical adsorption or a combination of them, while endothermic process is typical to chemical adsorption. The exothermic adsorption matched from the elucidation of the negative and large results of the entropy change (ΔS_{ads}°) in the attendance of *CME* is endothermic ($\Delta S_{ads}^{\circ} > 0$).

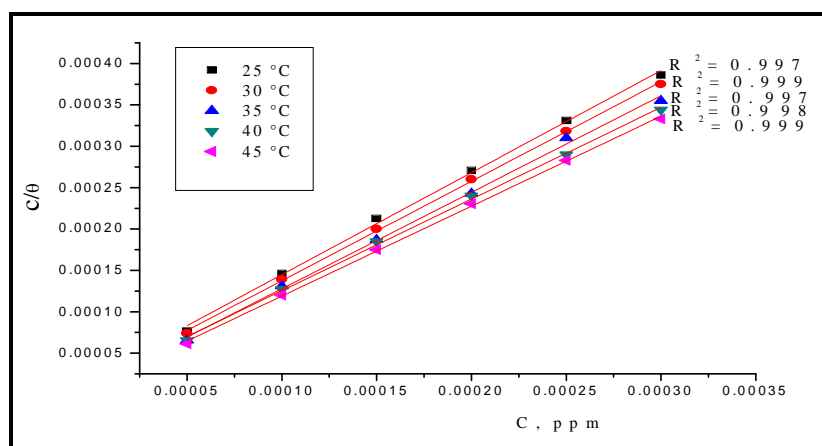


Figure 3. Langmuir adsorption graph for Al in 1M HCl solution including various doses of *CME* at different temperatures 298-318K.

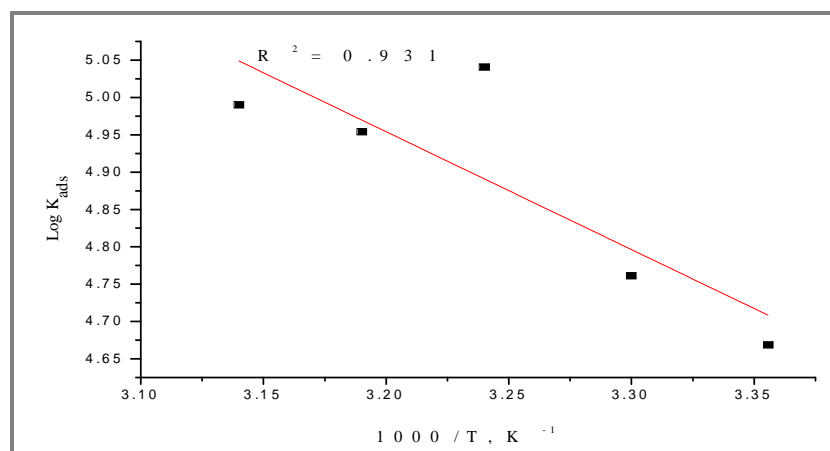


Figure 4. Graph of ($\log K_{ads}$) against ($1000/T$) for the dissolution of Al in 1M HCl solution + *CME*

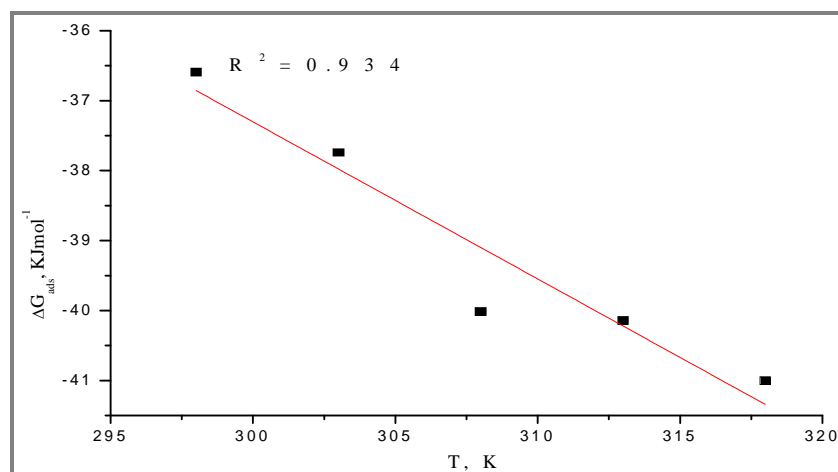


Figure 5. Graph of ΔG_{ads}° versus T for the adsorption of *CME* on Al surface in 1M HCl solution at various temperatures

Table 3. Adsorption parameters of *CME* for Al surface in 1M HCl solution resulted from Langmuir adsorption isotherm at various temperatures

Temp. (K)	K_{ads} , (ppm $\times 10^3$)	$-\Delta G_{ads}^{\circ}$ (kJ mol ⁻¹)	ΔH_{ads}° (kJ mol ⁻¹)	ΔS_{ads}° (J mol ⁻¹ K ⁻¹)
298	46.4	36.6		122.9
303	57.7	37.7		124.6
308	109.8	40.0	30.2	130.0
313	72.5	40.1		128.3
318	97.8	41.0		129.0

Effect of Temperature (Kinetic-Thermodynamic Parameters): At varied temperatures from 298 to 318 K in the presence of various doses of *CME*, WL procedure was applied. It was found that the raising in temperature is α with CR raising. With table 2, the CR of Al without *CME* raised sharply from 298 to 318 K, while with *CME* observed diminishing leading to raise in the protection efficiency (%IE). The activation parameters without and with *CME* in the temperature (298-318 K) is showed in table 4. The activation energy (Ea^*) for Al in 1 M HCl was assessed from the slope of the graphical representation by utilizing Arrhenius equation:

$$\log k = -Ea^*/2.303RT + \log A \quad \dots(10)$$

Where k refers the rate of dissolution, Ea^* refers the activation energy, R refers the universal gas constant, T refers the absolute temperature and A refers the Arrhenius pre-exponential factor [33]. The assessments of change in entropy (ΔS^*) and change in enthalpy (ΔH^*) can be assessed by utilizing the closest equation:

$$k_{corr} = [RT/Nh \exp (\Delta S^*/R) \exp (-\Delta H^*/RT)] \quad \dots(11)$$

Where k refers the dissolution rate, h refers the Planck's constant, N refers the Avogadro number, ΔS^* refers the entropy of activation and ΔH^* refers the enthalpy of activation. The negative outcomes of ΔS^* for the *CME* infer that that activated complex in the rate-determining step refers an association instead of dissociation step, signifying that a lack in disorder happens stratifying from reactants to the activated complex [34]. The negative sign of ΔH^* assured the exothermic process.

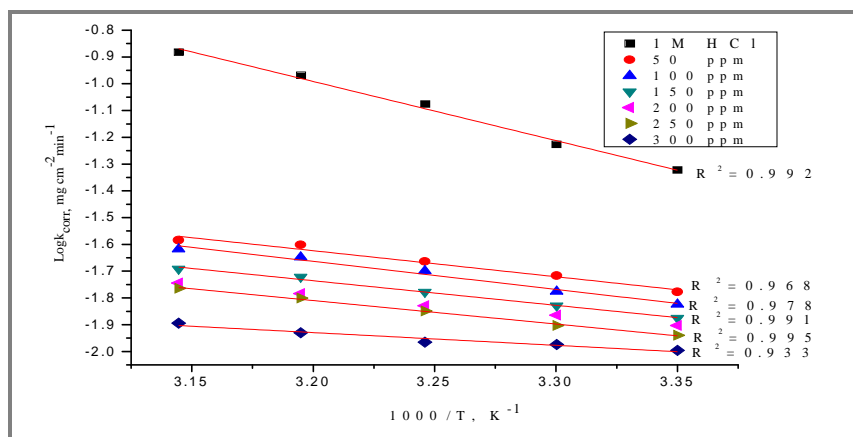


Figure 6. Arrhenius graph for dissolution rates (k_{corr}) of Al in 1M HCl solution in the presence and absence of various doses of CME.

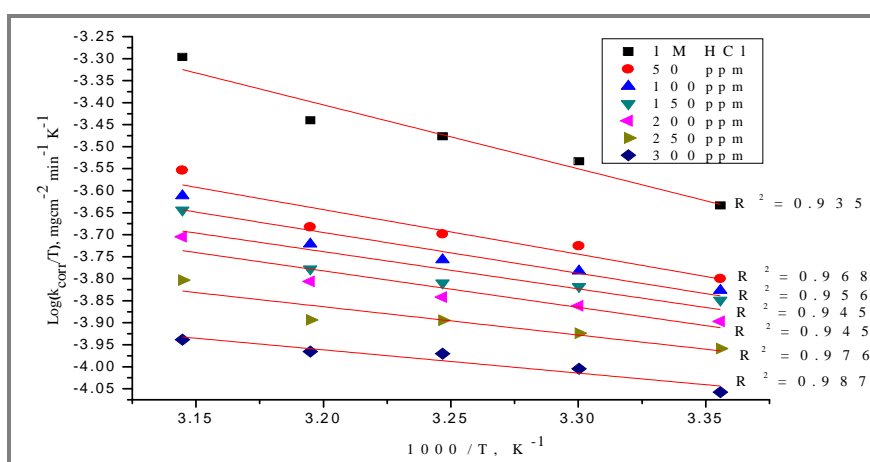


Figure 7. Graph of $\log(k_{corr}/T)$ against $(1000/T)$ of Al in 1M HCl (experimental solution) in the presence and absence of various doses of CME

Table 4. Kinetic-thermodynamic parameters for Al dissolution in the presence and absence of various doses of CME with the 1M HCl solution

Conc. (ppm)	Activation parameters		
	E_a^* kJ mol^{-1}	ΔH^* kJ mol^{-1}	$-\Delta S^*$ $\text{J mol}^{-1} \text{K}^{-1}$
Blank	73.2	21.3	106.9
50	20.0	8.1	220.4
100	18.6	7.4	222.7
150	17.6	6.8	226.3
200	14.4	6.5	230.9
250	10.5	3.6	254.3
300	9.1	3.5	256.2

Hydrogen Evolution assessments: Figure 8 can be reviewed viz, there is a linear correlation among volume of evolved H_2 gas and time. The average of liberated H_2 gas is restricted at the initiate of the reaction then raised with time passing substantially. By reason of Al is soluble in acidic aqueous medium with the release of hydrogen gas, the quantities of released H_2 gas in accordance with Al dissolution rate. The Al dissolution rate assessed from the slope of curve in attendance and non-attendance of inhibited acid solution. Adding CME restricted the rate of liberated H_2 gas with raising dose. The assessments of %IE are briefed in table 5 [21].

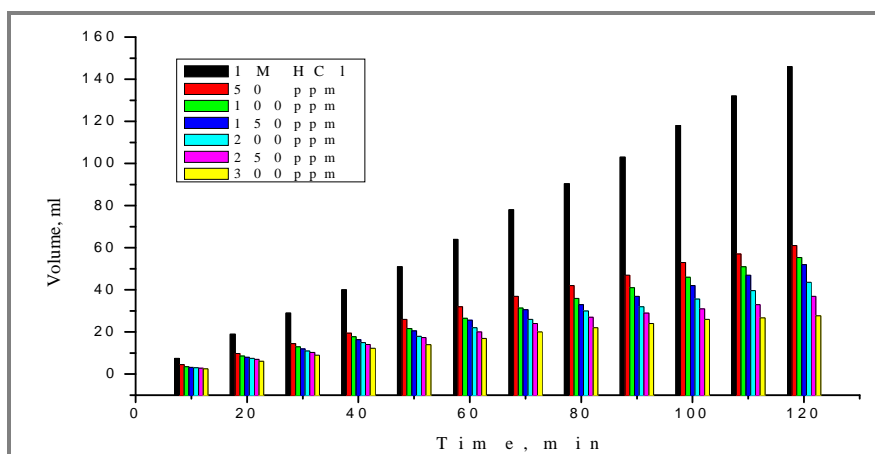


Figure 8. Variance of volume of H_2 gas evolved vs. time for Al dissolution in 1M HCl (experimental solution) in the presence and absence of various doses of CME at 298K

Table 5. Assessed values of corrosion rate and %IE for Al dissolution in 1M HCl solution including CME at 298K from Hydrogen evolution trial at 120 min

Conc. (ppm)	Corrosion rate ($mLmin^{-1}$) $\times 10^4$	%IE
Blank	12166	-
50	4733	61.1
100	4616	62.0
150	4500	63.0
200	3633	70.1
250	3400	72.0
300	2308	81.0

Acidification assessments: (H^+), was assessed in each case utilizing the closest equation:

$$pH = -\log[H^+] \quad \dots(12)$$

The CR of Al samples was assessed utilizing the closest equation:

$$CR \text{ (mole } dm^{-3} \text{ cm}^{-2} \text{ h}^{-1}) = \Delta H^+ / At \quad \dots(13)$$

Where $[\Delta H^+]$ is the variation between the first and last concentration of H^+ , A the surface area of sample in cm^2 and t , the time in hrs. The %IE was assessed utilizing the closest equation:

$$\%IE = 1 - ([H^+]_{inh} / [H^+]_{uninh}) \times 100 \% \quad \dots(14)$$

Where ΔH^+_{inh} and ΔH^+ are changes in H^+ concentration with and without the CME, separately. (Θ), was assessed utilizing the closest equation: [22]

$$\Theta = 1 - ([H^+]_{inh} / [H^+]_{uninh}) \quad \dots(15)$$

Tafel extrapolation curves: Tafel extrapolation curves for corrosion of Al was studied to examine the kind of the inhibitor (anodic, cathodic or mixed). Potentiodynamic polarization is a harmful DC technique but both EFM and EIS are AC technique. Tafel extrapolation curves are relation between current and potential. E_{corr} is the potential at which the oxidation potential and reduction potential are equal. Protection efficiency (IE) can be measured by taking tangent of anodic and cathodic curve and

point of meeting both of them fall it on the opposite axis this will give $\log i_c$, E_{corr} values. %IE measured by implementing in the following equation:

$$\%IE = [1 - (i_{\text{corr}} / i_{\text{corr}}^0)] \times 100 \quad \dots(16)$$

Table 6. Values of %IE for acidimetric method for CME at 298K

Conc. (ppm)	$\Delta H^+ \times 10^4$	θ	%IE
Blank	90.4	-	-
50	34.2	0.622	62.2
100	31.3	0.654	65.4
150	28.5	0.685	68.5
200	26.0	0.712	71.2
250	23.7	0.738	73.8
300	21.6	0.761	76.1

i_{corr} , i_{corr}^0 are the corrosion current densities of CME and 1M HCl (experimental solution), respectively. The analogous cathodic and anodic Tafel curve in figure 9 confirms the reduction and dissolution mechanism which show no change in the presence and absence of CME [35]. So, it could be deduced that CME is considered as mixed-kind inhibitor i.e. adsorbed on the cathodic sites of Al and diminishes the evolution of hydrogen gas. Moreover, the molecules of the extract adsorbed on anodic sites and diminish the anodic dissolution of Al [36, 37]. Values of E_{corr} slightly shift in trend of less negative. Tafel slopes don't change indicating that there is no change in the mechanism of the process and E_{corr} shift is less than 85 mV confirms mixed kind inhibitor.

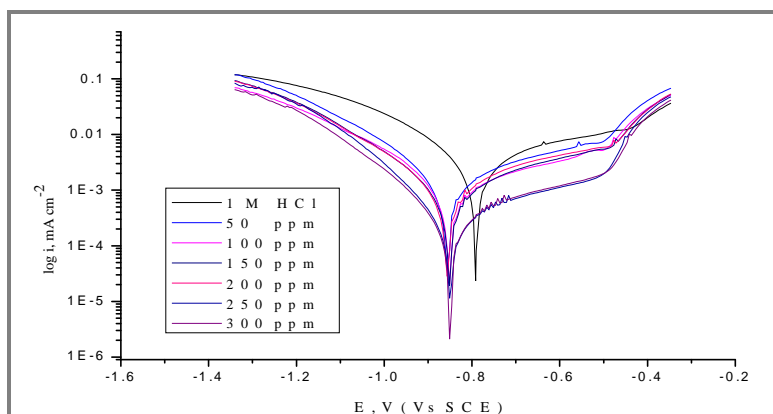


Figure 9. Potentiodynamic Polarization curve for corrosion of Al with and without different concentration of inhibitor

Table 7. Effect of CME doses on dissolution parameters of Al in 1M HCl solution at 298K

Conc. (ppm)	$-E_{\text{corr}}$ (mV vs. SCE)	i_{corr} (mA cm ⁻²)	β_a (mV dec ⁻¹)	β_c (mV dec ⁻¹)	C.R. (mpy)	θ	%IE
Blank	791	16.1	265	303	629.0	-	-
50	764	5.26	270	204	88.0	0.670	67.0
100	746	4.12	236	224	78.0	0.744	74.4
150	728	3.87	292	169	72.8	0.760	76.0
200	771	3.00	245	172	68.0	0.814	81.4
250	762	2.48	297	144	57.5	0.846	84.6
300	747	2.26	266	147	50.6	0.860	86.0

EIS Tests: Impedance is the power of measuring the resistance of a circle to the current flow. It may be estimated in the way of introducing AC potential and measure the current passed within the cell. The EIS device register the real (resistance) and imaginary (capacitance and inductance) elements of the impedance response of the system. EIS provides data that cannot be gained with DC techniques, can review systems in which multiple electrochemical reactions are processed and bring some insight into the capacitive characteristic of electrochemical cells. EIS has been confirmed to be a powerful and accurate procedure for measuring dissolution rates. Nyquist impedance spectra does not exhibit ideal semicircle which related to the frequency dispersion [38] due to roughness and the electrode surface heterogeneity. The Bode plots are distinguished by one time constant composed of large capacitive loop at high to medium frequency and inductive loop at down frequency. The capacitive loop at high frequencies clarifies the phenomenon relevant to the electric double layer. R_{ct} raises by raising the dose of the reviewed extract, so a decline in the dissolution rate. C_{dl} values diminish when the dose of plant extract raises. This drop in C_{dl} estimates is attributed to the gradual substituting of water molecules in the double layer by the adsorbed extract particulates which run down in the local dielectric constant of the metal solution interface and form a covering layer on the metal surface and diminishing the trend of dissolution reaction [39].

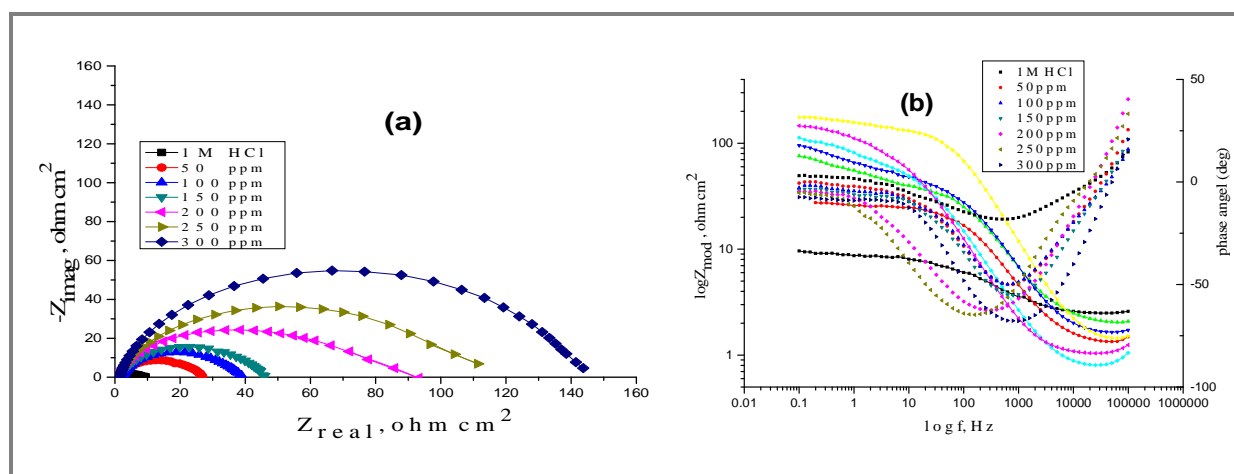


Figure 10. EIS Nyquist plots (a) and Bode plots (b) of Al in 1M HCl solution in presence and absence of various doses of CME at 298K.

Table 8. EIS parameters for the dissolution of Al in 1M HCl solution in the presence and absence of various doses of CME at 298K

Conc. (ppm)	$C_{dl} \times 10^5$ (F cm ⁻²)	R_{ct} (Ω cm ²)	θ	% IE
Blank	438	5.44	-	-
50	9.5325	15.98	0.660	66.0
100	8.6711	16.31	0.664	66.4
150	8.1499	16.82	0.677	67.7
200	7.8541	17.89	0.696	69.6
250	7.1894	21.84	0.751	75.1
300	6.6489	23.44	0.768	76.8

EFM Tests: EFM is a rapid and non-damaging technique, it draws a correlation between current and frequency without knowing of Tafel constants. It brings immediate information about (i_{corr}), this different from polarization technique (PP). The height [40] of the peaks is a measure for (i_{corr}) and from (i_{corr}) protection efficiency %IE was measured. In this technique frequency is applied and (i_{corr}) is evaluated. EFM is a non-linear response at which (i_{corr}) weakens in addition of doses of CME, by reason of (i_{corr}) is the current brought from dissolution so in case of CME should have little estimates table 9 shows the electrochemical parameters obtained from this technique. Causality factors [41]

(CF-2 and CF-3) make internal check about the validity of the assessments. Their estimates around 2, 3 and it is an evidence for validity of the results. The %IE increases by adding the extract and increases by increasing the extract dose.

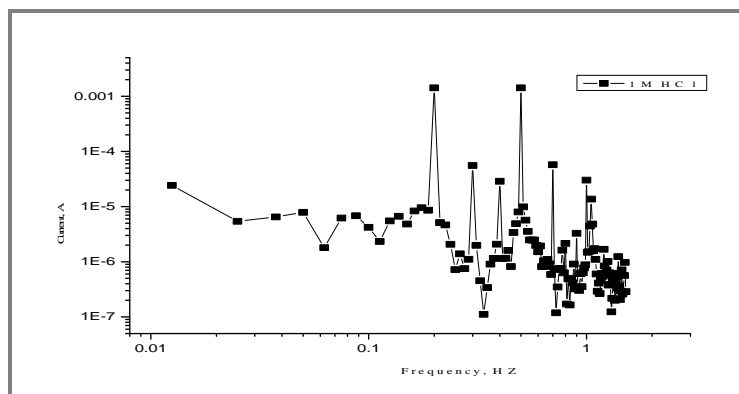


Figure 11. EFM spectrum for Al in 1M HCl (experimental solution) at 298K.

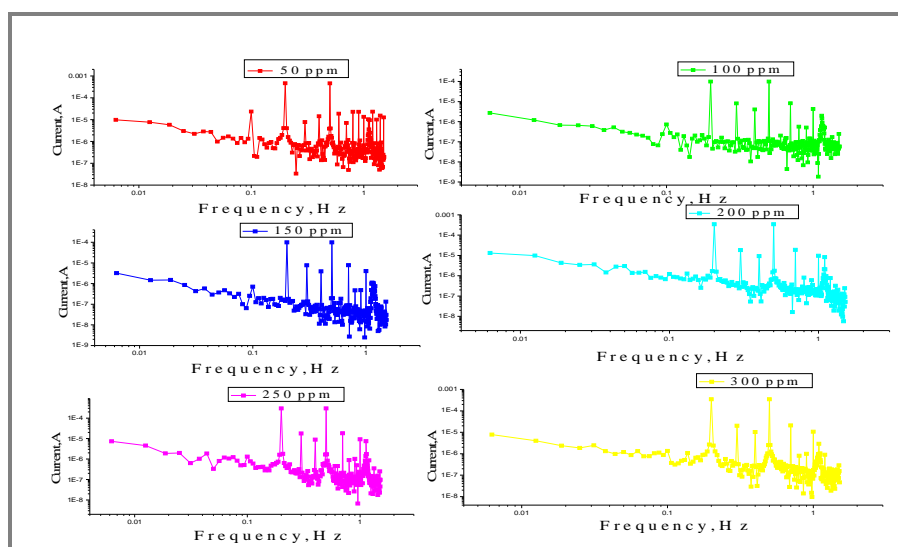


Figure 12. EFM spectra of Al dipped in solution of 1M HCl solution treated with various doses of CME at 298K.

Table 9. EFM data for dissolution of Al in 1M HCl solution containing various doses of CME at 298K

Conc. (ppm)	i_{corr} (μAcm^{-2})	β_a (mVdec^{-1})	β_c (mVdec^{-1})	CF -2	CF -3	C.R. (mpy)	θ	%IE
Blank	672.5	223	192	1.9	2.3	262.0	-	-
50	363.2	42	34	2.0	2.2	122.5	0.532	53.2
100	305.3	37	41	2.0	2.1	121.3	0.537	53.7
150	285.9	33	79	2.0	2.5	92.5	0.647	64.7
200	164.5	48	34	2.1	1.9	89.0	0.660	66.0
250	161.1	69	79	2.0	2.5	69.3	0.735	73.5
300	154.7	39	29	2.0	2.3	69.0	0.737	73.7

FT-IR Analysis: Analysis appears that there is a peak at 670 cm^{-1} refers to sulphate ion (SO_4^{2-}) / (C-Br) // (OH) out of plane bend, a peak at 1078 cm^{-1} refers to skeletal vibration (C-C) / (C-O stretch) of ester // primary amine stretch /// (C=S) thio carbonyl, peak at 1231 cm^{-1} refers to (C-O) of sulphate ester, a peak at 1400 cm^{-1} refers to carboxylate group, peak at 1637 cm^{-1} refers to (C-O) of (CONH_2) amide group/ alkenyl (C=C), a peak at 2091 cm^{-1} refers to cumulated system (C=C=O) / (-NCS)

isothiocyanate group, a peak at 2599 cm^{-1} refers to thiol SH stretch, a peak at 3448 cm^{-1} refers to phenolic / alcoholic (OH) group, two peaks at 3750 cm^{-1} , 3905 cm^{-1} due to crystallization of water [42-47].

ATR Analysis: A peak at 762 cm^{-1} refers to (C-H) aromatic or skeletal vibration (C-C) out of plane bend. There is a disappearance of three peaks 1078 cm^{-1} , 1231 cm^{-1} and 2599 cm^{-1} and there are two new peaks one at 1540 cm^{-1} refers to aromatic (C=C) / secondary amine, the second at 1747 cm^{-1} refers to (CO) of ester / (CO) of carboxyl refers to dissociation of the ester already exist into carboxyl and alcoholic OH. There are four shifts; 1st shift is of carboxylate group from 1400 cm^{-1} to 1419 cm^{-1} , 2nd shift is of (CO) of (CONH₂) amide group/ alkyl (C=C) from 1637 cm^{-1} to 1650 cm^{-1} , 3rd shift is of cumulated system (C=C=O) / (-NCS) isothiocyanate group from 2091 cm^{-1} to 2083 cm^{-1} and 4th shift is of phenolic / alcoholic (OH) group from 3448 cm^{-1} to 3382 cm^{-1} (Figure 13).

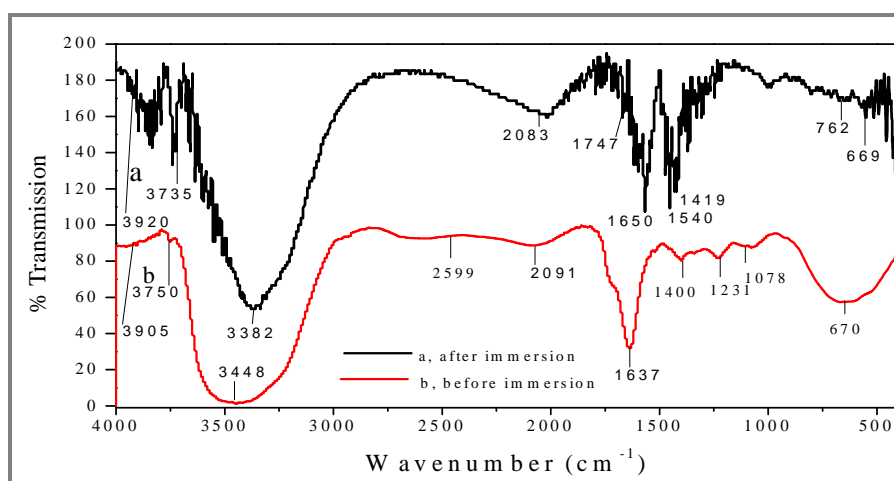


Figure 13. (a) Aluminum ATR-FTIR spectra after dipping in 1M HCl solution + 300 ppm of CME, (b) pure CME before immersion

UV Spectroscopy:

Before immersion: There are four bands; 1st at 308 nm refers to phenolic structure (benzonitrile), 2nd at 291 nm refers to aromatic amino acid/ cyclohexane // phenanthrene, 3rd at 266 nm refers to (C=C-C=N-N-CONH₂)/ iso propene, and 4th at 216 nm refers to α , β unsaturated ketone / ring (diene) // peptide bond /// (R-SO-R) [48-50].

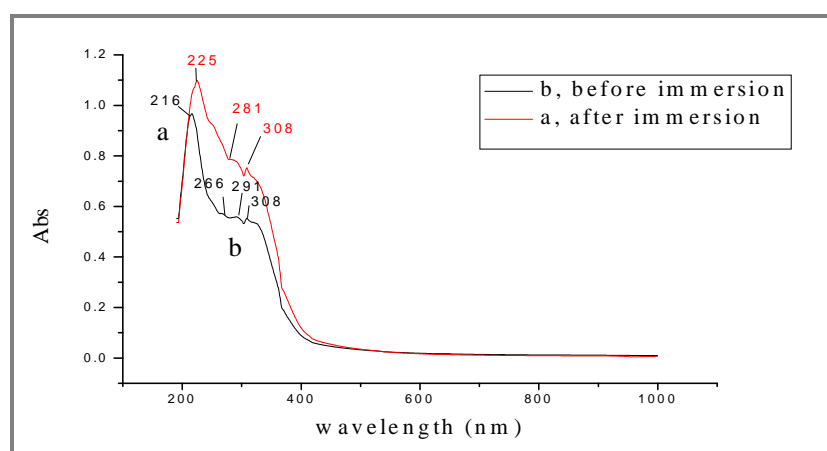


Figure 14. (a) UV/Visible spectra of CME solution (b) the experimental solution containing CME after immersion of Al coupons for 24 hours

After immersion: There are three bands 1st at 308 nm phenolic structure (benzonitrile), 2nd at 281nm refers to (-C=N-NH-CO-NH₂)/ (RNO₂)/ (RCOCL), 3rd at 225 nm refers to α , β unsaturated diene ester/ (R-SO-R). There are four bands in the pure plant extract and three bands in the analysis after immersion for 24 h and this means a disappearance of one band and this is in a good agreement with ATR analysis in terms of disappearance and formation of new peak (Figure 14).

AFM Studies: Assessment the roughness of metal superficies and providing images with highly resolute covering survey can be gained by AFM. The three-dimensional (3D), two-dimensional (2D) AFM micrographs for Al surface in 1M HCl (experimental solution) with and without *CME* table 10, the data tell that Al surface submerged in 1M HCl (experimental solution) whole a day is more than the inhibited Al in surface roughness assessment, which reveals that Al sample is acutely deteriorated due to the corrosive medium. The average rough of Al sample in attendance of *CME* was diminished to 431.6 nm these parameters tell that the surface become soft. The softness of the surface is by reason of setting up of a condensed protective film of the *CME* on the metal surface, hence protecting the Al surface from successive deterioration (Table 11).

Table 10. Three-dimensional (3D) + two-dimensional (2D) AFM pics of the relaxed Al surface immersed in 1M HCl solution and in solution with 300 ppm *CME*

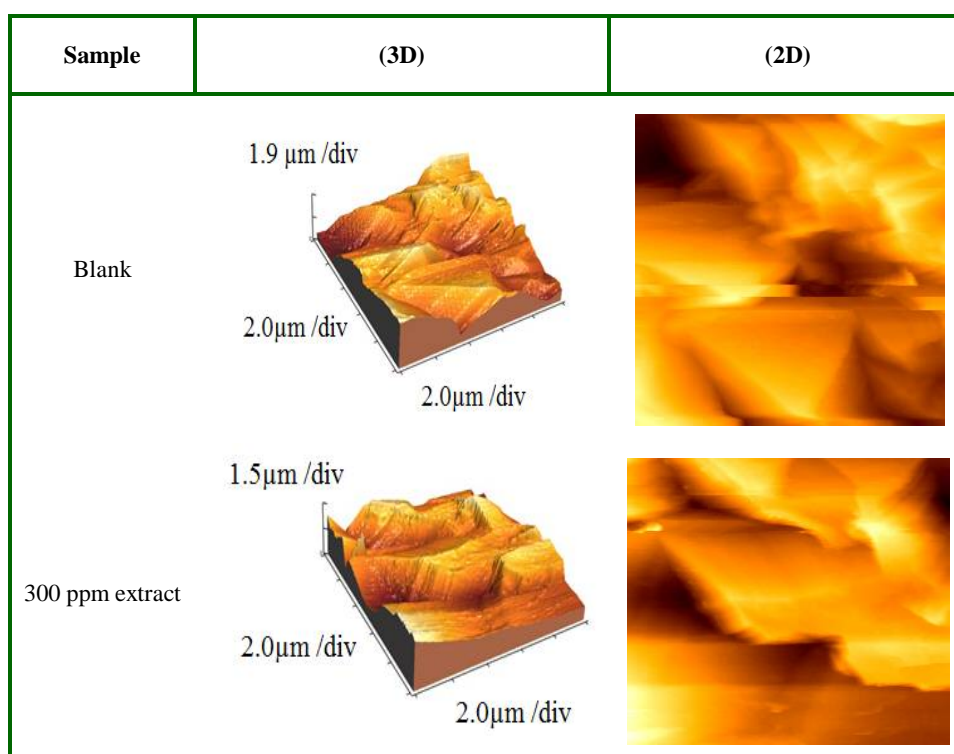


Table 11. AFM assessments for Al surface in presence and absence of *CME*

Sample	Ave rough (Ra) nm	Rms rough nm(Rq)	The peak valley height (Rp) μm
Blank	667.1	825.0	2.910
<i>Cerumium rubrum</i>	431.6	523.8	1.500

Where: Rms rough (Root- mean- squared roughness), (Rq).Ave rough (Average roughness), R_a, R_p= peak valley high.

Biological Activity: The results of table 12 exhibited that *CME* has suitable effect against bacterial growth, so the corrosion rate diminished.

Table 12. Bacteria colonies cultivated in Petri dishes assessed by Doc-it colony counter device for blank of bacteria compared with pure and 300 ppm of CME

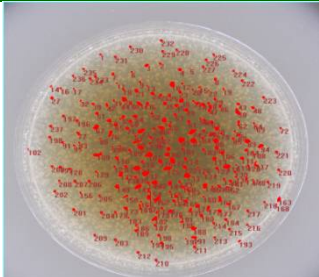
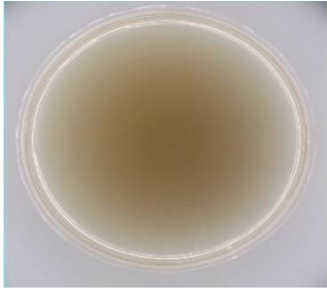
No.of colonies	Counting by Doc-ti colony device
Blank's No. of colonies is 241	
Pure and 300 ppm CME the same result 0 colony	

Table 13. Comparison between % IE of some plant extracts used as corrosion inhibitors for Al in 1 M HCl at 25°C

Source	Metal/Medium	IE	Ref.
<i>Eucalyptus citriodora</i>	Al /MS / 1M HCl	64	51
<i>Cnidoscopus aconitifolius</i>	Al /1M HCl	37	52
<i>Caricapapaya Leaves</i>	Al/1M H ₂ SO ₄	72	53
<i>Thymus algeriensis extract</i>	2024 Al alloy/1MHCl	79	54
<i>Raphia hookeri</i>	Al/1MHCl	56	55
<i>Breadfruit peel</i>	Al/0.5MH ₂ SO ₄	85	56
<i>Pawpaw leaves</i>	Al/1MHCl	84	57
<i>Commiphora pedunculata (CP)gum</i>	AA3001/1MHCl	73	58
<i>Pyrazoloantiazamide derivatives</i>	Al/2MHCl	78	59
<i>Novel phthalocyanines</i>	Al/0.1MHCl	83	60
<i>Chondria Macrocarpa (CME)</i>	Al/1 M HCl	86.0	Our result

Table 13 shows a comparison of some plant extracts used as inhibitors for Al in HCl medium. As shown from the table the CME extract used in this paper can be used as inhibitor for Al in HCl acid Solution and it will be good inhibitor by increasing its concentration.

APPLICATION

The presence of this extract can be used as inhibitor for other metals at different media and can be tried as corrosion inhibitor in industry

CONCLUSION

1. The adsorption of extracts depends on their doses, temperatures and the natural of the extract and metal.
2. EIS results exhibited that a progress in the R_{ct} and a diminish in C_{dl} .

3. The adsorption of the examined plant extract on Al surface in 1M HCl solution obeys Langmuir adsorption isotherm.
4. A surface film of extract on the metal surface is obtained via sharing or transferring charge from the extract molecules into the vacant orbitals on the metal surface (chemisorption) or due to electrostatic attraction forces between the protonated extract molecules and the negatively charged metal surface due to the adsorption of the Cl⁻ anions on the positively charged Al surface (physisorption).
5. The present obtainable measured values of non-electrochemical and electrochemical technique are perfect and highly valid. *CME* acts as good inhibitor to protect Al against the dissolution in corrosive solutions compared to other plant extracts.
6. It was found that *CME* has no effect against bacteria growth and hence the corrosion rate decreased.

REFERENCES

- [1]. N. Raghavendra, J. I. Bhat, Anti-corrosion Properties of Areca Palm Leaf Extract on Aluminum in 0.5 M HCl Environment, *S. Afr. J. Chem.*, **2018**, 71, 30–38.
- [2]. A. Ennouri, A. Lamiri, M. Essahli, Corrosion Inhibition of Aluminum in Acidic Media by Different Extracts of *Trigonellafoenum-graecum* L Seeds. *Port. Electroch. Acta*, **2017**, 35(5), 279-295.
- [3]. O. Olawale, B. J. O. Ogundipe, S. Julius, T. Siji, Optimisation and modeling of Aluminum corrosion inhibition using Almond (*prunus amygdalus*) fruit Leaves extract as green inhibitor in HCl acidic medium, *IJMET*, **2018**, 9(13), 1274–1285.
- [4]. A. O. James, O. Akaranta, Corrosion inhibition of aluminum in 2.0 M hydrochloric acid solution by the acetone extract of red onion skin, *Afr. J. Pure Appl. Chem.*, **2009**, 3(12), 262-268.
- [5]. A. M. El-Azaly, Influence of Soybean (*Glycine Max*) Plant Extract on Corrosion of Aluminum in 1M HCl, *Int. J. Electrochem. Sci.*, **2019**, 14, 2714-2731.
- [6]. H. Imane, E. Mohamed, L. Abdeslam, Inhibition of Al Corrosion in 0.1 M Na₂CO₃ by *Mentha pulegium*. *Port. Electrochim. Acta*, **2019**, 37(6), 335-344.
- [7]. B. Kasuga, E. Park, R. L. Machunda, Inhibition of Aluminum Corrosion Using *Carica papaya* Leaves Extract in Sulphuric Acid, *JMMCE*, **2018**, 6, 1-14.
- [8]. N. Raghavendra, J. I. Bhat, Protection of Aluminum Metal in 0.5 M HCl Environment by Mature Arecanut Seed Extracts: A Comparative Study by Chemical, Electrochemical and Surface Probe Screening Techniques, *J. Phys. Sci.*, **2018**, 29(1), 77–99.
- [9]. R. Narasimha, I. B. Jathi, Red Arecanut Seed Extract as a Sustainable Corrosion Inhibitor for Aluminum Submerged in Acidic Corrodent: An Experimental Approach Towards Zero Environmental Impact. *Period. Polytech. Chem. Eng.*, **2018**, 62(3), 351-358.
- [10]. N. Raghavendra, L. V. Hublikar, S. M. Patil, P. J. Ganiger, A. S. Bhinge, Efficiency of sapota leaf extract against aluminum corrosion in a 3 M sodium hydroxide hostile fluid atmosphere: a green and sustainable approach, *Bull. Mater. Sci.*, **2019**, (42), 226, 1-11.
- [11]. H. Hachelef, A. Benmoussat, A. Khelifa, D. Athmani, D. Bouchareb, Study of corrosion inhibition by Electrochemical Impedance Spectroscopy method of 5083 aluminum alloy in 1M HCl solution containing propolis extract, **2016**, 7 (5), 1751-1758.
- [12]. O. U. Abakedi, Aluminum Corrosion Inhibition by *Micro desmispuberula* Leaf Extract in 2 M Hydrochloric Acid Solution, *Int. J. Inno. Scientific and Eng. Tech. Res.*, **2017**, 5(3), 6-14.
- [13]. A. C. Mary, K. S. Suruthi *Chrysanthemum* Flower Extract as a Green Inhibitor for Aluminum Corrosion in Alkaline Medium, *Int. J. Chemtech Res.*, **2018**, (11)7, 37-44.
- [14]. L. Eladio, V. Guillen, Prospective of the aluminum industry in venezuela and its role in building sustainable future, *Ecodiseno and sostenibilidad*, **2011**, 3(1), 175-191.
- [15]. I. J. Polmear, Light alloys: metallurgy of the light metals. 3rd edition, **1995**, 1-362.
- [16]. M. Kumar, U. Shankar, Evaluation of Mechanical Properties of Aluminum Alloy 6061- Glass Particulates reinforced Metal Matrix Composites, *IJMERE*, **2012**, 2(5), 3207-3209.

- [17]. A. S. Fouda, K. Shalabi, A. El-Hossiany, Moxifloxacin Antibiotic as Green Corrosion Inhibitor for Carbon Steel in 1 M HCl, *J. Bio Tribo Corros.*, **2016**, 2,18.
- [18]. K.Singh, K. K.Agrawal, V.Mishra, U. S.Mubeen, A. Shokla, A review on: *Thevetia peruviana*. *Int Res J Pharm.*, **2012**, 3(4), 74 –77.
- [19]. R. H. Furneaux, T. T. Stevenson, The xylogalactan sulfate from Chondriamacrocarpa Ceramiales, Rhodophyta, *Hydrobiologia*, **1990**, 204, 615-620.
- [20]. A. S. Fouda, A. M. El-Wakeel, K. Shalabi and A. El-Hossiany, Corrosion Inhibition for Carbon Steel by Levofloxacin Drug in Acidic Medium, *J. Elixir Corrosion and Dye*, **2015**, 83, 33086-33094.
- [21]. E. I.Ating, S. A.Umoren, I. I.Udousoro, E. E.Ebenso, A. P. Udoh, Leaves extract of Ananas sativum as green corrosion inhibitor for aluminum in hydrochloric acid solutions, *Green Chem Lett Rev.*, **2010**, 3(2), 61-68.
- [22]. S. O. Adejo, S. G.Yiase, L. Leke, M.Onuche, M. V. Atondo, T. T. Uzah, Corrosion studies of mild steel in sulphuric acid medium by acidimetric method, *Int.J.Corros.Scale Inhib.*, **2019**, 8(1), 50-61.
- [23]. A. S. Fouda, A. El-Hossiany, H. Ramadan, Corrosion Inhibition of Rumex Vesicarius Extract on Stainless Steel 304 in Hydrochloric Acid, *IJRASET*, **2017**, 5, 1698-1710
- [24]. A. Nithya, P. Shanthi, N. Vijaya, R. J. Rathish, S. S.Prabha, R. M.Joany, S.Rajendran, Inhibition of corrosion of aluminum by an aqueous extract of beetroot (Betanin), *Int. J. Nano. Corros. Sci. Eng.*, **2015**, 2(1), 1-11.
- [25]. M. M. Motawe, A.El-Hossiany, A. S. Fouda, Corrosion Control of Copper in Nitric Acid Solution using Chenopodium Extract, *Int. J. Electrochem. Sci.*, **2019**, 14, 1372-1387.
- [26]. N. Nnaji, N. Nwaji, J. Mack, T. Nyokong, Corrosion Resistance of Aluminum against Activation: Impact of Benzothiazole-Substituted Gallium Phthalocyanine, *Molecules*, **2019**, 24 (207), 1-22.
- [27]. A. S. Fouda, A. El-Hossiany, H. Ramadan, Calotrpicsprocera plant extract as green corrosion inhibitor for 304 stainless steel in hydrochloric acid solution, *Zastita Materijala*, **2017**, 58(4), 541-555
- [28]. M. M.Fares, A. K. Maayta, M. M. Al-Qudah, Pectin as promising green corrosion inhibitor of aluminum in hydrochloric acid solution, *Corros. Sci.*, **2012**, 60, 112–117.
- [29]. A. Khadraoui, A. Khelifa, K. Hachama, R. Mehdaoui, Thymus algeriensis extract as a new eco-friendly corrosion inhibitor for 2024 aluminum alloy in 1 M HCl medium, *J. Mol. Liquids*, **2016**, 214, 293–297.
- [30]. K. O.Abiola, Y. Tobunb, Cocos Nucifera L. water as green corrosion inhibitor for acid corrosion of aluminum in HCl solution, *Chinese Chem. Lett.*,**2010**, 21(12), 1449–1452.
- [31]. X.Li, S.Deng, Inhibition effect of *Dendrocalamus brandisii* leaves extract on aluminum in HCl, H₃PO₄ solutions, *Corros. Sci.*, **2012**, 65, 299–308.
- [32]. D. Y.Silvère, B. K.Valery, K. M.Guy-Richard, O.Augustin, T.Albert, Cefadroxil Drug as Corrosion Inhibitor for Aluminum in 1 M HCl Medium: Experimental and Theoretical Studies, *JAC.*,**2018**, 11 (4), 24-36.
- [33]. A. S. Fouda, H. Ibrahim, S. Rashwaan, A. El-Hossiany, R. M. Ahmed, Expired Drug (pantoprazole sodium) as a Corrosion Inhibitor for High Carbon Steel in Hydrochloric Acid Solution, *Int. J. Electrochem. Sci.*, **2018**, 13, 6327 – 6346.
- [34]. M. N. El-Haddad, A. S. Fouda, Electroanalytical, quantum and surface characterization studies on imidazole derivatives as corrosion inhibitors for aluminum in acidic media, *J MOL LIQ.*, **2015**, 209, 480-486.
- [35]. A. S. Fouda, S. A. Abd El-Maksoud, A. A. M. Belal, A. El-Hossiany, A. Ibrahim, Effectiveness of Some Organic Compounds as Corrosion Inhibitors for Stainless Steel 201 in 1M HCl: Experimental and Theoretical Studies, *Int. J. Electrochem. Sci.*, **2018**, 13, 9826-9846.
- [36]. A. I. Ali, N. Foaud, Inhibition of aluminum corrosion in hydrochloric acid solution using black mulberry extract, *J. Mater. Environ. Sci.*, **2012**, 3(5), 917-924.

- [37]. I. O. Arukalam, N. T. Ijomah, S. C. Nwanonenyi, H. C. Obasi, B. C. Aharanwa, P. I. Anyanwu, Studies on acid corrosion of aluminum by a naturally occurring polymer (Xanthan gum), *IJSER.*, **2014**, 5(3), 663-673.
- [38]. A. Nithya, P. Shanthi, N. Vijaya, R. R. Joseph, P. S. Santhana, R. M. Joany, S. Rajendran, Inhibition of Corrosion of Aluminum by An Aqueous Extract of Beetroot (Betanin)., *Int. J. Nano. Corr. Sci. Engg.*, **2015**, 2(1), 1-11.
- [39]. A. Singh, I. Ahmad, M. A. Quraishi, Piper longum extract as green corrosion inhibitor for aluminum in NaOH solution, *Arab J Chem.*, **2016**, 9, S1584 -S1589.
- [40]. R. W. Bosch, J. Hubrecht, W. F. Bogaerts, B. C. Syrett, Electrochemical frequency modulation: a new electrochemical technique for on-line corrosion, *Corrosion*, **2001**, 57(1), 60–70.
- [41]. A. S. Fouda, S. Rashwan, A. El-Hossiany, F. E. El-Morsy, Corrosion Inhibition of Zinc in Hydrochloric Acid Solution using some organic compounds as Eco-friendly Inhibitors, *JCBPS*, **2018**, 19(1), 001-024
- [42]. P. O. Ameh, Inhibitory action of albiziazygia gum on mild steel corrosion in acid medium, *Afr.J.Pure Appl.Chem.*, **2014**, 8(2), 37- 46.
- [43]. E. F. Neves, L. H. C. Andrade, Y. R. Suarez, S. M. Lima, W. F. Antonialli-Junior, Age-related changes in the surface pheromones of the wasp *Mischocyttarus consimilis* (Hymenoptera: Vespidae), *Genet. Mol. Res.*, **2012**, 11(3), 1891-1898.
- [44]. J. J. P. Paul, Screening of phytochemicals of blechnum orientale l. collected from kothiyar, kanyakumari district, Tamil Nadu, *India. IAJPS*, **2018**, 5(3), 1671-1674.
- [45]. Petchiammal, S. Selvaraj, The corrosion control of Al using lawsonia inermis seed extract in acid medium. *Int.J.Chem. Tech. Res.*, **2013**, 5(4), 1566-1574.
- [46]. I. P. Sari, Y. Yulizar, Green synthesis of magnetite (Fe₃O₄) nanoparticles using *Graptophyllum pictum* leaf aqueous extract, *IOP Conf. Ser.: Mater. Sci. Eng.*, **2017**, (191), 1-5.
- [47]. A. S. Fouda, M. Abdel Azeem, S. A. Mohamed, A. El-Hossiany, E. El-Desouky, Corrosion Inhibition and Adsorption Behavior of Nerium Oleander Extract on Carbon Steel in Hydrochloric Acid Solution, *Int. J. Electrochem. Sci.*, **2019**, 14, 3932–3948.
- [48]. A. Petchiammal, S. Selvaraj, Influence of cassia alata leaves on Aluminium in 1.0N hydrochloric acid, *Carib. J.Sci. Tech.*, **2013**, 1, 123-130.
- [49]. G. T. Xavier, B. Thirumalairaj, M. Jaganathan, Effect of piperidin-4-ones on the corrosion inhibition of mild steel in 1 N H₂SO₄, *Int.J.Corros.*, **2014**, 2015, 1-16.
- [50]. R. S. Nathia, S. Perumal, M. Moorthy, V. Murugesan, R. Rangappan, V. Raj, Synthesis, characterization and inhibition performance of schiff bases for Aluminium corrosion in 1 M H₂SO₄ solution, *J Bio TriboCorros.*, **2020**, 6(5), 1-15.
- [51]. M. A. Ezeokonkwo, P. O. Ukoha, N. J. N. Nnaji, Green inhibitor for aluminium and mild steel in Acidic media: a case study of exudates of *Eucalyptus citriodora*, *Int. J. Chem. Sci.*, **2012**, 10(3), 1365-1373.
- [52]. B. U. Ugi, I. E. Uwah, N. U. Ukpe., Inhibition and Adsorption impact of Leave Extracts of *Cndoscolus aconitifolius* on Corrosion of Aluminium Sheet in 1 M HCl Medium, *J. Appl. Sci. Environ. Manage*, **2014**, 18 (2), 319-325.
- [53]. B. Kasuga, E. Park, R. L. Machunda, Inhibition of Aluminium Corrosion Using *Carica papaya* Leaves Extract in Sulphuric Acid, *Journal of Minerals and Materials Characterization and Engineering*, **2018**, 6, 1-14.
- [54]. A. B. Khadraoui, A. Khelifa, H. Boutoumi, B. Hammouti, *Mentha pulegium* extract as a natural product for the inhibition of corrosion. Part I: electrochemical studies, *Natural Product Research*, **2014**, 28(15), 1206–1209.
- [55]. S. A. Umoren, I. B. Obot, E. E. Ebenso, N. O. Obi-Egbedi, The Inhibition of aluminium corrosion in hydrochloric acid solution by exudate gum from *Raphia hookeri*, *Desalination*, **2009**, 247, 561–572.
- [56]. K. J. Orie, M. Christian, The Corrosion Inhibition of Aluminium Metal In 0.5M Sulphuric Acid Using Extract of *Breadfruit* Peels, *Int. Res. J. Eng. Technol.*, **2015**, 2 (8), 1.
- [57]. M. Omotoma, O. D. Onukwuli, Evaluation of *Pawpaw* leaves extract as anticorrosion agent for Al in hydrochloric acid medium, *Nigerian Journal of Technology*, **2017**, 36 (2), 496–504.

- [58]. P. O. Ameh, N. O. Eddy, Theoretical and experimental studies on the corrosion inhibition potentials of 3-nitrobenzoic acid for mild steel in 0.1 M H₂SO₄, *Cogent Chemistry*, **2016**, 2, 1-18.
- [59]. A. S. Fouda, F. M. El-Taweel, M. Elgamil, Corrosion Inhibition of Aluminum in Hydrochloric Acid Solution Using Some Pyrazolocarbothioamide Derivatives, *Int. J. Electrochem. Sci.*, **2017**, 12, 11397–11418.
- [60]. O. K. Ozdemir, A. Aytac, D. Atilla, M. Durmus, Corrosion inhibition of Al by novel phthalocyanines in hydrochloric acid solution, *J. Mater. Sci.*, **2011**, 46, 752–758.